7. Welcher, A. A., Suter, U., De Leon, M., Snipes, G. J. & Shooter, E. M. A myelin protein is encoded by the homologue of a growth arrest-specific gene. *Proc. Natl Acad. Sci. USA* **88,** 7195–7199 (1991).
8. Schaeren-Wiemers, N., Valenzuela, D. M., Frank, M. & Schwab, M. E. Characterization of a rat gene, rMAL, encoding a protein with four transmembrane domains in central and peripheral myelin. *J. Neurosci.* **15,** 5753–5764 (1995).
9. Caroni, P. & Schwab, M. E. Two membrane protein fractions from rat central myelin with inhibitory properties for neurite growth and fibroblast spreading. *J. Cell Biol.* **106,** 1281–1288 (1988).
10. Schwab, M. E. & Thoenen, H. Dissociated neurons regenerate into sciatic but not optic nerve explants in culture irrespective of neurotrophic factors. *J. Neurosci.* **5,** 2415–2423 (1985).
11. Chen, M., Schnell, L., van der Haar, M., Oertle, T. & Schwab, M. Inhibitory activity and domain(s) of the myelin protein Nogo-A. *Soc. Neurosci. Abstr.* **25,** 2030 (1999).
12. Roebroek, A. J. *et al.* Cloning and expression of alternative transcripts of a novel neuroendocrine-specific gene and identification of its 135-kDa translational product. *J. Biol. Chem.* **268,** 13439–13447 (1993).
13. Wieczorek, D. F. & Hughes, S. R. Developmentally regulated cDNA expressed exclusively in neural tissue. *Brain Res. Mol. Brain Res.* **10,** 33–41 (1991).
14. Ninkina, N. N., Baka, I. D. & Buchman, V. L. Rat and chicken s-rex/NSP mRNA: nucleotide sequence of main transcripts and expression of splice variants in rat tissues. *Gene* **184,** 205–210 (1997).
15. Geisler, J. G., Stubbs, L. J., Wasserman, W. W. & Mucenski, M. L. Molecular cloning of a novel mouse gene with predominant muscle and neural expression. *Mamm. Genome* **9,** 274–282 (1998).
16. Roebroek, A. J. *et al.* Genomic organization of the human NSP gene, prototype of a novel gene family encoding reticulons. *Genomics* **32,** 191–199 (1996).
17. Morris, N. J., Ross, S. A., Neveu, J. M., Lane, W. S. & Lienhard, G. E. Cloning and preliminary characterization of a 121 kDa protein with multiple predicted C2 domains. *Biochim. Biophys. Acta* **1431,** 525–530 (1999).
18. Nagase, T. *et al.* Prediction of the coding sequences of unidentified human genes. X. The complete sequences of 100 new cDNA clones from brain which can code for large proteins in vitro. *DNA Res.* **5,** 169–176 (1998).
19. Rubin, B. P., Dusart, I. & Schwab, M. E. A monoclonal antibody (IN-1) which neutralizes neurite growth inhibitory proteins in the rat CNS recognizes antigens localized in CNS myelin. *J. Neurocytol.* **23,** 209–217 (1994).

Acknowledgements

We thank T. Oertle and C. Bandtlow for suggestions and discussions; T. Flego for technical assistance; R. Schöb and E. Hochreutener for help with the Figures; and C. Brösamle for critically reading the manuscript. This study was supported by grants from the Swiss National Science Foundation, the Maurice E. Muller Foundation (Berne), the International Research Institute for Paraplegia (Zurich) and the Spinal Cord Consortium of the Christopher Reeve Paralysis Foundation (Springfield, New Jersey).

Correspondence and requests for materials should be addressed to M.E.S.

Identification of the Nogo inhibitor of axon regeneration as a Reticulon protein

Tadzia GrandPré*†, Fumio Nakamura*†, Timothy Vartanian‡ & Stephen M. Strittmatter*§

** Department of Neurology, and §Section of Neurobiology, Yale University School of Medicine, New Haven, Connecticut, USA*
‡ Department of Neurology, Beth Israel Deaconess Medical Center, Harvard Institutes of Medicine, Boston, Massachusetts, USA
† These authors contributed equally to this work

Adult mammalian axon regeneration is generally successful in the peripheral nervous system (PNS) but is dismally poor in the central nervous system (CNS). However, many classes of CNS axons can extend for long distances in peripheral nerve grafts[1]. A comparison of myelin from the CNS and the PNS has revealed that CNS white matter is selectively inhibitory for axonal outgrowth[2]. Several components of CNS white matter, NI35, NI250(Nogo) and MAG, that have inhibitory activity for axon extension have been described[3–7]. The IN-1 antibody, which recognizes NI35 and NI250(Nogo), allows moderate degrees of axonal regeneration and functional recovery after spinal cord injury[8,9]. Here we identify Nogo as a member of the Reticulon family, Reticulon 4-A. Nogo is expressed by oligodendrocytes but not by Schwann cells, and associates primarily with the endoplasmic reticulum. A 66-residue lumenal/extracellular domain inhibits axonal extension and collapses dorsal root ganglion growth cones. In contrast to Nogo, Reticulon 1 and 3 are not expressed by oligodendrocytes, and the 66-residue lumenal/extracellular domains from Reticulon 1, 2 and 3 do not inhibit axonal regeneration. These data provide a molecular basis to assess the contribution of Nogo to the failure of axonal regeneration in the adult CNS.

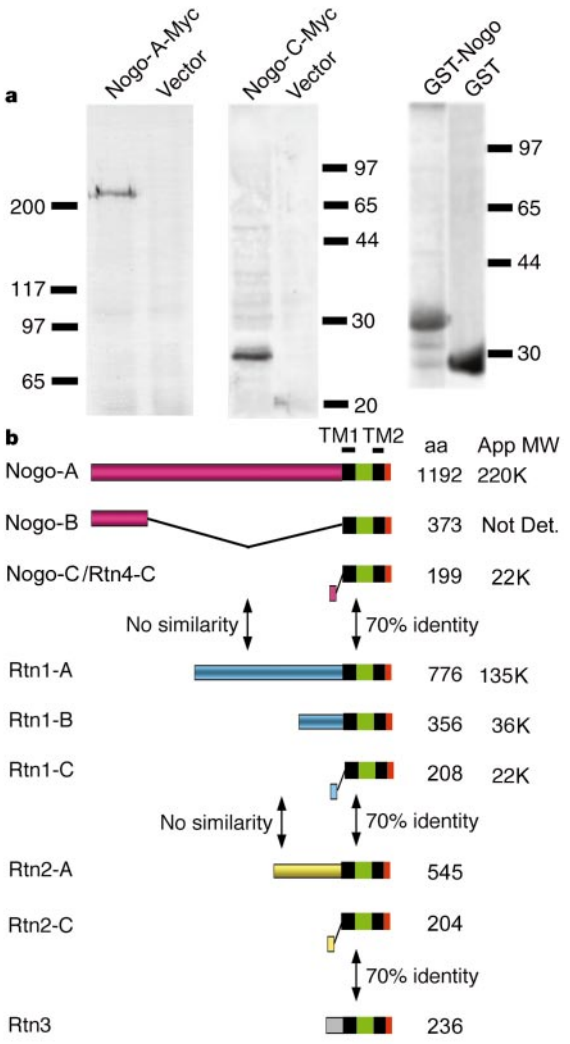

Figure 1 Identification of Nogo. **a**, Membrane extracts from HEK293T cells transfected with vector alone or with an expression vector encoding Nogo-A–Myc or Nogo-C–Myc were analysed by Myc immunoblot (left two panels). The apparent relative molecular mass of Nogo-A–Myc is 225K and that of Nogo-C–Myc is 25K. The purity of the GST–Nogo fusion protein is illustrated by Commassie Blue staining of SDS–PAGE samples (right panel). **b,** The structure of predicted protein sequences and their relationship to one another. Suffixes A, B and C refer to different splice forms of each family member. The abbreviations are Rtn 1 (Reticulon 1, or neuro-endocrine-specific protein, NSP), Rtn2 (or NSP-like gene 1, NLG1) and Rtn3 (or NSP-like gene 2, NLG2). GenBank accession numbers for the protein sequences: Nogo-A, BAA47909; Nogo-B, AAD31021; Nogo-C, AAF01564; Rtn1-A, A46583; Rtn1-B, I60903; Rtn1-C; I60904; Rtn2-A, 5032055; Rtn2-B; AAC32544; Rtn3, 5174655.

The sequence of six peptides derived from a proteolytic digest of presumed bovine NI250(Nogo) protein has been published[5], and the probable full-length complementary DNA sequence for this protein has been deposited in the GenBank. This 4.1-kilobase (kb) human cDNA clone, KIAA0886, is derived from the Kazusa DNA Research Institute effort to sequence random high molecular-weight brain-derived cDNAs[10]. This cDNA clone encodes a protein of relative molecular mass 135,000 (M_r 135K) that matches all six of the peptide sequences derived from bovine Nogo.

The predicted molecular mass of protein derived from this clone does not match the observed 200K–250K mobility of Nogo by SDS-polyacrylamide gel electrophoresis (PAGE) (Fig. 1; refs 4, 5). However, the protein has a high number of charged residues that might alter its mobility in gel electrophoresis. Therefore, we measured the electrophoretic mobility of a Myc-epitope tagged version of KIAA0886-derived protein expressed in HEK293T cells. Myc immunoreactivity is detectable with an apparent size in the 225K range under reducing conditions (Fig. 1). Thus, the cDNA directs the expression of a protein with appropriate electrophoretic mobility and the amino-acid sequence to be Nogo. We call this protein hNogo-A (Fig. 1).

The C-terminal third of the hNogo-A sequence shares high homology with the Reticulon (Rtn) protein family (Fig. 1). Reticulon1 has also been called neuro-endocrine specific protein (NSP) because it is expressed exclusively in neuro-endocrine cells[11]. All Rtn proteins share a 200-amino-acid residue region of sequence similarity at the C terminus of the protein[11–15]. Related sequences have been recognized in the fly and worm genomes[14]. This region is ~70% identical across the Rtn family. Amino-terminal regions are not related to one another and are derived from various alternative RNA splicing events. From analysis of sequences deposited in the GenBank and by homology with published Rtn1 isoforms, we predict three forms of the Nogo protein. Nogo-B (M_r 37K) may possibly correspond to NI35, and explain the antigenic relatedness of the NI35 and NI250 axon outgrowth-inhibiting activity. Nogo-C-Myc has an electrophoretic mobility of 25K by SDS–PAGE and has been described previously as Rtn4-C and vp20 (ref. 15) (Fig. 1).

The conserved C-terminal tail of the Rtn family proteins contains two hydrophobic domains separated by a 66-residue hydrophilic segment (Fig. 2). None of the sequences contains a signal peptide. The predicted topology for these proteins is for the N and C termini to reside in the cytosol, and for the conserved region to associate with the lipid bilayer. For Rtn1-A, experimental evidence shows that the polypeptide behaves as an integral membrane protein, and that the hydrophobic segments of the conserved domain are responsible for this behaviour[11]. Myc-tagged Nogo is also associated with particulate fractions and is extracted by detergent but not high

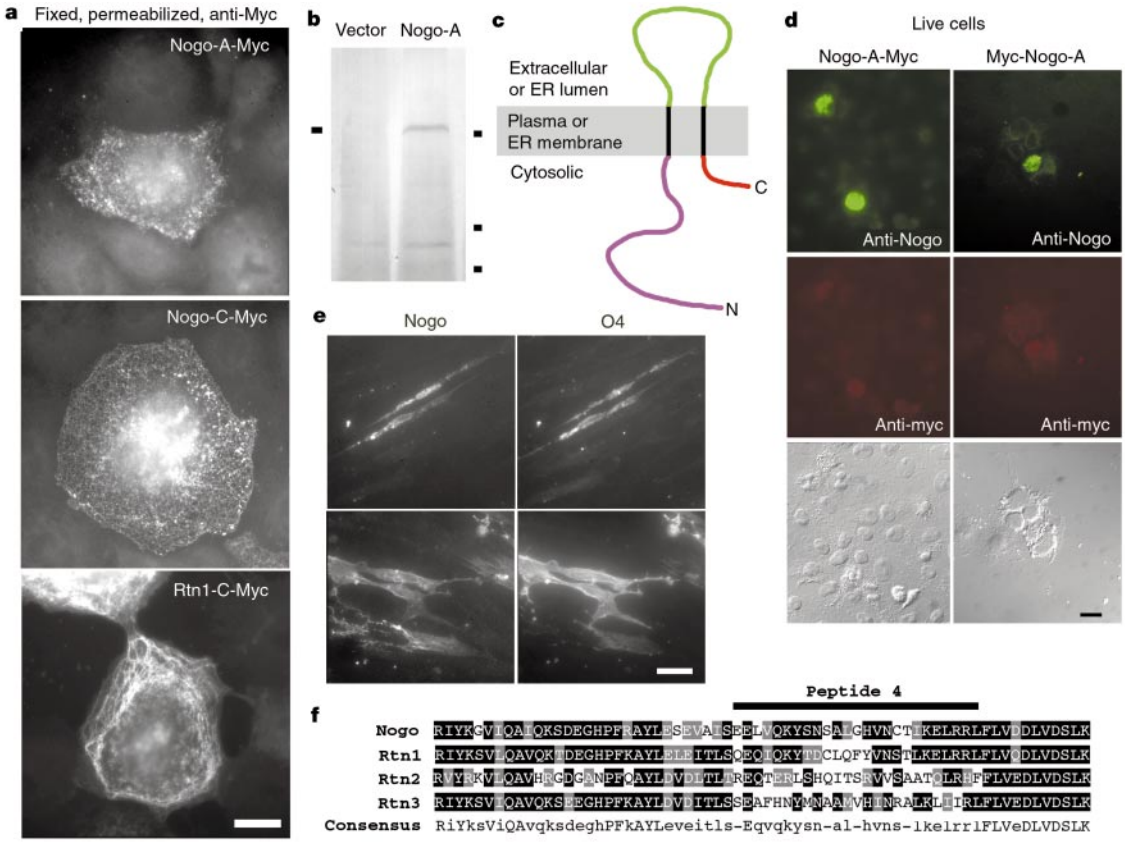

Figure 2 Topology of Nogo protein in transfected COS-7 cells. **a**, COS-7 cells were transfected with plasmids directing the expression of either Nogo-A or Nogo-C or Rtn1-C with a Myc-epitope tag at the C terminus. Thirty-six hours after transfection, cells were fixed and stained for total Myc immunoreactivity after permeabilization. Note the reticular pattern of staining for each of the three proteins. Scale bar, 70 μm. **b**, HEK293T cells were transfected with control plasmid or a plasmid directing the expression of full-length Nogo-A. Protein was analysed by immunoblot with an antibody generated by immunization of rabbits with the GST–Nogo protein. Nogo is indicated on the left. Markers of 200K, 116K and 97K are shown on the right. **c**, Model of the predicted structure for the Rtn family of proteins. Nogo and Rtns associate with the ER membrane and, to a lesser extent, with the plasma membrane. Green represents the 66-residue predicted lumenal/extracellular loop; red, the C terminus; black, the two hydrophobic segments; and purple, the alternatively spliced N-terminal domain. **d**, COS-7 cells prepared as in **a** were incubated with anti-Nogo and anti-Myc primary antibodies before fixation and incubation with secondary fluorescent antibodies. The three panels on the left or on the right are views of the same field showing cell-surface NI-250, cell-surface Myc epitope and differential interference contrast (DIC) imaging. Note that the epitope recognized by the anti-GST–Nogo antibody is detectable on the cell surface of some cells but that the Myc epitope is not, regardless of whether the epitope is at the N terminus (Myc–Nogo-A) or the C terminus (Nogo–A-Myc) of the protein. The very low level of rhodamine fluorescence in these cells is due to non-specific antibody staining and bleed-through from the fluorescein channel. The percentage of cells exhibiting surface Nogo reactivity was significantly less than the total percentage of transfected cells detected in **a**. The specificity of the anti-Nogo staining was verified by the total absence of staining in vector-transfected cells and by blockade of staining in the presence of GST–Nogo antigen (not shown). Scale bar, 150 μm. **e**, Unfixed, live chick spinal cord explants were double-stained at 4° with the anti-GST–Nogo antibody (left) and with the O4 oligodendrocyte-specific monoclonal antibody (right). Note the coincident staining of several oligodendrocytes in each pair of panels amongst numerous unstained astrocytes. Anti-Nogo staining was undetectable when GST–Nogo antigen was included in the primary antibody incubation (not shown). Scale bar, 150 μm. **f**, Amino-acid sequence corresponding to the entire predicted lumenal/extracellular loop for each of the proteins shown in Fig. 1.

ionic strength (data not shown). When overexpressed in kidney cells, the Rtn1 protein is localized primarily in the endoplasmic reticulum (ER) in a finely granulated pattern, hence the Reticulon name[11]. There is a di-lysine ER retention motif at the C terminus of Nogo and most Rtns[15,16]. In neurons, Rtn1 is expressed throughout processes and is concentrated in growth cones[17]. Its localization in transfected kidney cells has led to the suggestion that Rtn1 might regulate protein sorting or other aspects of ER function[11]. Both the A and C splice forms of Nogo exhibit a reticular distribution when expressed in COS-7 cells, which is similar to that of Rtn1-C (Fig. 2).

The predicted intramembrane topology of the two hydrophobic domains of Nogo suggests that the 66 amino acids between these segments might be localized to the lumenal/extracellular face of the membrane (Fig. 2). To explore this further, we generated an antiserum directed against the 66-residue domain (Fig. 2). The antibody detects a low level of surface expression of this epitope, and a Myc epitope at the N or C terminus of expressed Nogo is not detected unless cells are permeabilized (Fig. 2). We attribute this surface staining to a minority of Nogo protein associated with the plasma membrane rather than the ER membrane. These data support a topographic model wherein the N and C termini of the protein reside in the cytoplasm and 66 residues of the protein protrude on the lumenal/extracellular side of the ER or plasma membrane.

If Nogo is a major contributor to the axon outgrowth inhibitory characteristics of CNS myelin as opposed to PNS myelin[4,5,8], then Nogo should be expressed in adult CNS myelin but not PNS myelin. Northern blot analysis of Nogo expression was carried out using probes derived from the 5′ Nogo-A/B-specific region and from the 3′ Nogo common region of the cDNA. A single band of ~4.1 kb was detected with the 5′ probe in adult rat optic nerve total RNA samples, but not in sciatic nerve samples (Fig. 3). The results indicate that the Nogo-A clone is probably a full-length cDNA and are consistent with Nogo functioning as a CNS-myelin-specific axon outgrowth inhibitor. Northern blot analysis with a 3′ probe showed that optic nerve expresses high levels of the Nogo-A messenger RNA and much lower levels of Nogo-B and Nogo-C. Whole brain expresses both Nogo-A and -C, but a number of peripheral tissues (including sciatic nerve) express little or no Nogo (Fig. 3). Nogo-C/Rtn4-C expression has been found in skeletal muscle and adipocytes, as well as in brain[15]. Within the Rtn family, optic-nerve expression appears to be selective for Nogo, with no detectable expression of Rtn 1 or Rtn 3 (Fig. 3). Reticulon 2 has not been examined. *In situ* hybridization reveals Nogo mRNA in cells with the morphology of oligodendrocytes in adult rat optic nerve and pyramidal tract (Fig. 3). Within the brain, Nogo expression is also detected in certain neuronal populations. In contrast to Nogo, Rtn1 and Rtn3 are not expressed in optic nerve but mRNA is detected in certain neuronal populations.

We analysed Nogo protein localization in spinal-cord explant cultures treated with platelet-derived growth factor (PDGF) and low serum to induce oligodendrocyte differentiation, using the anti-Nogo antibody and the oligodendrocyte-specific O4 monoclonal antibody. In living cells, both the lumenal/extracellular 66-residue loop of Nogo and the O4 antigen are detected on the surface of oligodendrocytes (Fig. 2e). About half the O4-positive cells in these cultures show Nogo surface staining.

The expression of recombinant Nogo in HEK293T cells allows a rigorous test of whether this protein has axon outgrowth-inhibiting effects. Washed membrane fractions from vector- or hNogo-A–Myc-transfected HEK293T cells were added to chick E12 dorsal root ganglion (DRG) explant cultures. Growth cone morphology was assessed after a 30-min incubation at 37° by fixation and rhodamine–phalloidin staining (Fig. 4). The control HEK membranes have no detectable effect on growth cone morphology. The Nogo-A-containing membrane fractions induce the collapse of most DRG growth cones. This growth cone collapse suggests Nogo-A inhibits axon outgrowth activity, and Nogo inhibition of axon extension can also be shown (see below). The Nogo-C form also exhibits collapse activity, indicating that the shared C terminus of the protein, including the hydrophobic segments and the 66-residue lumenal/extracellular domain, contains functionally important residues. Additional inhibitory activity in the N-terminal region of Nogo-A is not excluded by these studies. The sensitivity of more immature explant cultures from E10 chick embryos (Fig. 4) or from E15 rat embryos (data not shown) is substantially less. The developmental regulation of sensitivity is consistent with experiments using partially purified Nogo[18].

In the growth-cone-collapsing Nogo-C protein, the hydrophilic 66-residue lumenal/extracellular domain seems more likely than the membrane-embedded hydrophobic domains to interact with the surface of DRG neurons. To test this hypothesis, the 66-residue region of hNogo was expressed in and purified from *Escherichia coli*. Most of the glutathione *S*-transferase (GST)–Nogo fusion protein accumulates in inclusion bodies, but can be recovered by urea

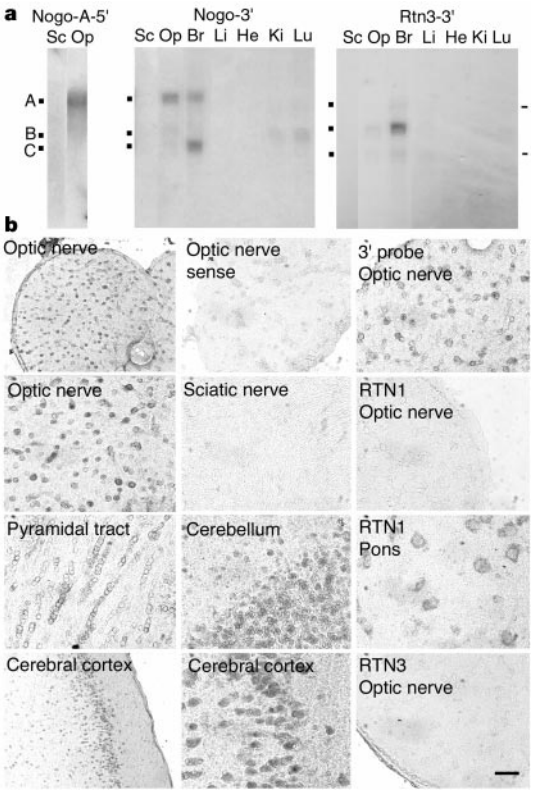

Figure 3 Localization of Nogo mRNA to oligodendrocytes. **a**, Total RNA from the indicated rat tissues was extracted, separated on a formaldehyde–agarose gel and transferred to a nylon membrane. Equal loading was verified by ethidium bromide staining of the 28S and 18S ribosomal RNA (mobility indicated at right). A 5′ fragment of hNogo-A complementary to both Nogo-A and -B, or a 3′ fragment of hNogo-A complementary to all Nogo mRNA splice forms was used to generate a radioactive probe for Nogo. The migration of the A, B and C splice forms is indicated at left. A similar analysis for the Rtn3 mRNA is shown in the right panel. Sc, sciatic nerve; Op, optic nerve; Br, brain; Li, liver; He, heart; Ki, kidney; Lu, lung. **b**, The distribution of various mRNAs was analysed in adult rat nervous system by *in situ* hybridization with digoxegenin-labelled riboprobes. Left and middle columns, probes complementary to the 5′ end of the Nogo gene (splice forms A and B) were hybridized. Top right panel, an antisense probe corresponding to the 3′ of the Nogo (splice forms A, B and C) was used. Bottom three panels of the right column, probes complementary to Rtn1C and Rtn 3 mRNAs were used, as indicated. All riboprobes were antisense, except in the panel marked 'sense'. Scale, 200 μm in all panels except the top and bottom left panels (scale bar, 400 μm). Note the expression of Nogo in cells with the appearance of oligodendrocytes in the optic nerve and in the pyramidal tract. Rtn1 and Rtn3 are not expressed in optic nerve. Some neurons express Nogo.

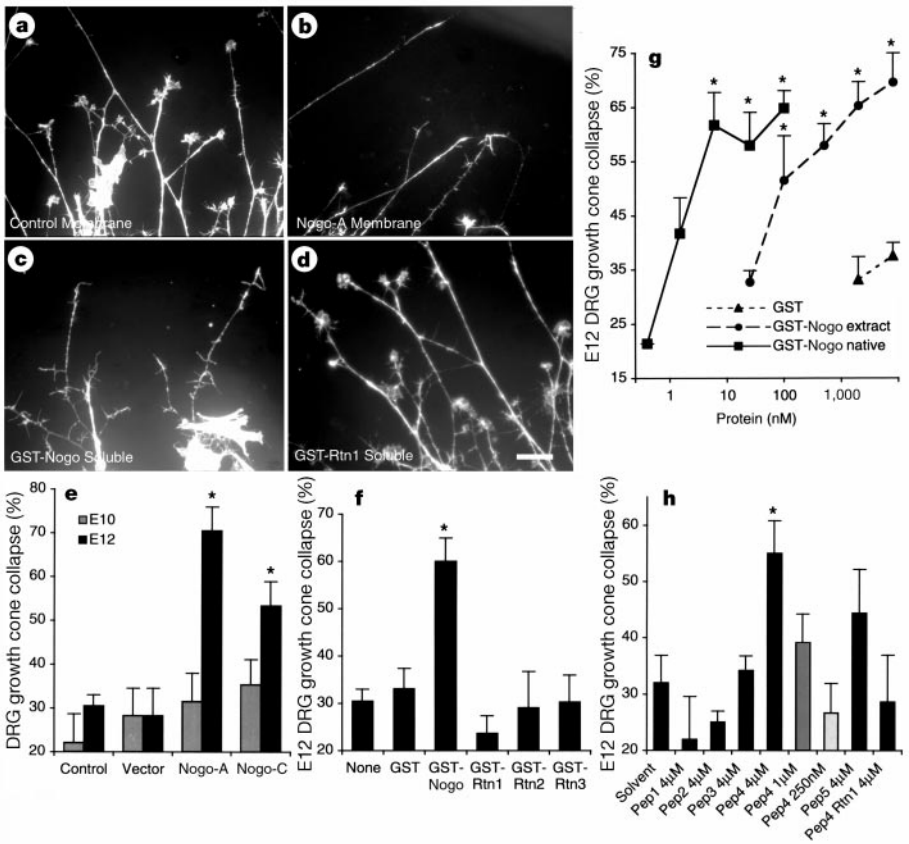

Figure 4 Nogo collapses axonal growth cones. **a**–**d**, Chick E12 DRG explants were cultured and growth cone collapse was assessed as described in Methods. Cultures were exposed to the following preparations for 30 min before fixation and staining with rhodamine–phalloidin: vector-transfected HEK293T cell membrane fraction at 0.2 mg total protein/ml (**a**); pcDNA3.1-NogoA–Myc vector-transfected HEK293T cell membrane fraction at 0.2 mg total protein ml^{-1} (**b**); 25 nM native GST–Nogo protein (**c**); and 25 nM native GST–Rtn1 protein (**d**). **e**–**h**, Results from growth cone collapse assays as in **a**–**d** are quantitated. All results are the means ± s.e.m. from 4–7 determinations. Membranes were prepared from vector-transfected or Nogo expression plasmid-transfected HEK293T cells and tested at 0.2 mg total protein ml^{-1} with either E10 or E12 DRG explant cultures (**e**). Native GST and GST fusion proteins were tested at 25 nM (**f**), and native and urea extracted fusion proteins were assayed at various concentrations (**g**). Peptides corresponding to portions of the 66-residue lumenal/extracellular fragment of Nogo or Rtn1 were tested at the indicated concentrations. Pep1, residues 1–25; Pep2, 11–35; Pep3, 21–45; Pep4, 31–55; Pep5, 42–66 (**h**). Those values significantly different from control are indicated (asterisk, $P < 0.05$, Student's two-tailed t test).

extraction. This restricted region of Nogo possesses potent (median effective concentration (EC_{50}) = 50 nM) growth-cone-collapsing activity for chick E12 DRG neurons (Fig. 4). The urea-extracted protein preparation is likely to present only a small fraction of the Nogo sequence in an active conformation. Therefore, we purified the 10% of GST–Nogo that is soluble in *E. coli* using a glutathione-Sepharose resin. This preparation is even more potent than the urea-extracted protein as a collapsing factor, acutely altering growth cone morphology at concentrations as low as 1 nM. The nanomolar potency is on a par with most known physiologic regulators of axon guidance. Axon outgrowth from DRG neurons and nerve growth factor (NGF)-differentiated PC12 cells is also blocked by this soluble GST–Nogo protein in nanomolar concentrations (Fig. 5). When GST–Nogo is bound to substrate surfaces, axonal outgrowth from DRG neurons or PC12 cells is reduced to undetectable levels (Fig. 5). These are selective effects on axon outgrowth rather than cell survival as GST–Nogo does not reduce the number of neurofilament-positive adherent cells (137 ± 24% of GST-treated cultures) nor significantly alter the number of apoptotic nuclei identified by DAPI (4′,6-diamidino-2-phenylindole dihydrochloride) staining (4.0 ± 1.7% in control cultures and 5.2 ± 1.1% in GST–Nogo-treated specimens).

Oligodendrocytes appear to express Nogo selectively amongst the Rtns. To explore the selectivity of Nogo's role in the inhibition of axonal regeneration, we considered whether other Rtns exert axon outgrowth-inhibiting activity. The predicted 66-residue lumenal/extracellular fragments of Rtn1, 2 and 3 were expressed as GST fusion proteins and purified in native form. At concentrations in which the Nogo fragment collapses most E12 DRG growth cones, the other Rtns do not alter growth cone morphology (Fig. 4). Thus, the axon regeneration inhibiting activity is specific for Nogo in the Rtn family.

To further define the active domain of Nogo, 25-residue peptides corresponding to segments of the 66-residue sequence were synthesized. The peptide corresponding to residues 31–55 of the extracellular fragment of Nogo exhibits growth-cone-collapsing (Fig. 4) and outgrowth-inhibiting (Fig. 5) activities at concentrations of 4 μM. Although this sequence may provide the core of the inhibitory domain, the 66-residue fragment is clearly required for full potency. Notably, this is the region within the 66-residue domain that shares the least similarity to other Rtn proteins (Fig. 2e), consistent with the other family members being inactive as axon-regeneration inhibitors. Indeed, the 31–55-residue lumenal/extracellular peptide of Rtn1 exerts no growth-cone-collapsing activity (Fig. 4).

We have identified Nogo as an oligodendrocyte-specific member of the Rtn family and have shown that a discrete domain of Nogo can inhibit axon outgrowth. Other Rtns do not possess this activity. The expression of Nogo in oligodendrocytes but not Schwann cells may contribute to the failure of axonal regeneration in the adult mammalian CNS as opposed to in the adult PNS. The relative contribution of Nogo as compared with other CNS myelin components to the non-permissive nature of CNS white matter can now

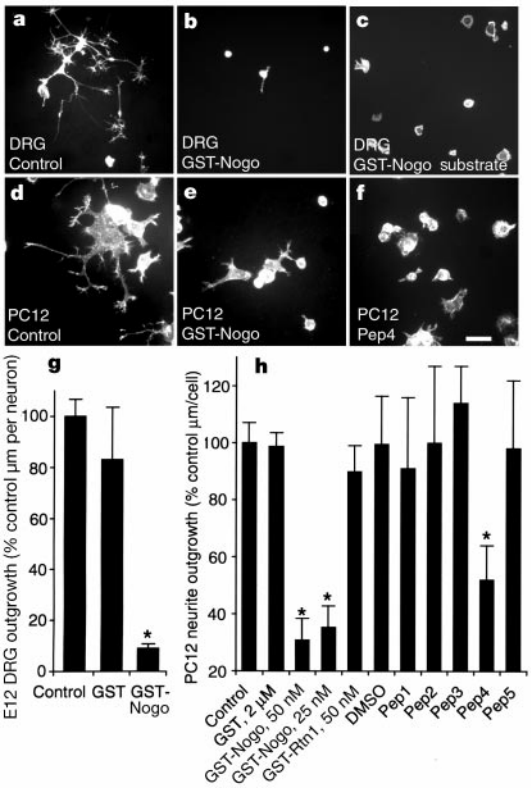

Figure 5 The lumenal/extracellular domain of Nogo inhibits neurite outgrowth. **a**–**f**, Chick E12 dissociated DRG neurons (**a**–**c**) or NGF-differentiated PC12 cells (**d**–**f**) were cultured for 10–24 hours in the presence of the indicated proteins or peptides: no added protein (**a**); 100 nM native GST–Nogo protein (**b**); GST–Nogo substrate coating (10 ng protein dried per mm^2) (**c**); 2 μM GST protein (**d**); 25 nM native GST–Nogo protein (**e**); and 4 μM peptide 4 (residues 31–55 of the Nogo lumenal/extracellular domain) (**f**). A substrate coating of GST (50 ng protein dried per mm^2) did not alter outgrowth from control levels (data not shown). Neurite outgrowth was visualized by staining with rhodamine–phalloidin. Scale bar, 200 μm. **g**–**h**, Results from neurite outgrowth assays as in **a**–**f** are quantitated**.** For dissociated E12 DRG cultures tested with soluble proteins, the GST concentration was 2 μM and the native GST–Nogo concentration was 100 nM (**g**). For NGF-differentiated PC12 cultures, the protein concentrations are indicated and the peptide concentrations were 4 μM (**h**). The peptide sequences are as in Fig. 4. All results are the means ± s.e.m. from 4–7 determinations. Those values significantly different from control are indicated (asterisk, $P < 0.05$, Student's two-tailed t test).

be characterized at a molecular level. For example, axonal regeneration in mice lacking Nogo can be compared with that in mice lacking MAG or both MAG and Nogo. IN-1 effects can be studied in animals lacking Nogo expression to determine whether the effect of the IN-1 antibody is due to Nogo blockade. Although the current data are consistent with a role for Nogo in blocking adult CNS axonal regeneration after pathologic injury, this may or may not be related to the physiologic role of Nogo in non-pathologic states. On the basis of localization studies, other Rtns are thought to have a role in ER function[11]. Most of Nogo is distributed in a reticular pattern in COS-7 cells, and only a minority seems to be accessible at the cell surface. Nogo is found on the surface of some, but not all, oligodendrocytes. The localization of at least part of Nogo's axon outgrowth-inhibiting activity to a discrete region of the protein should facilitate further mechanistic analysis of axon repulsion by this protein. □

Methods

Expression vectors and protein purification

The full-length sequence of Nogo-A (KIAA0886) was generously provided by the Kazusa DNA Research Institute. The full-length coding sequence was amplified by polymerase chain reaction (PCR) and ligated into the pcDNA3.1–MycHis vector (Invitrogen) to generate a plasmid encoding Nogo-A fused at the C terminus to the Myc epitope (Nogo-A–Myc). Alternatively, the coding sequence was amplified using primers that encode an in-frame Myc epitope immediately N-terminal to the first residue and a stop codon at the C terminus (Myc–Nogo-A). The Nogo-C–MycHis and Rtn1C–MycHis expression vectors were derived in the same fashion except that an adult rat brain cDNA library was used as a template for the PCR reaction with primers based on the Nogo-C or Rtn1C sequences[11].These plasmids were transfected into COS-7 or HEK293T by the Lipofectamine (Life Sciences) or the FuGENE 6 (Boerhinger Mannheim) method.

A portion of Nogo-A encoding the 66-residue lumenal/extracellular fragment of Nogo-A (Fig. 2e) was amplified by PCR and ligated into the pGEX-2T plasmid to yield a prokaryotic expression vector for the GST–Nogo fusion protein. Similar regions of Rtn1, Rtn2 and Rtn3 were amplified by nested PCR using an adult rat brain cDNA library as template and were ligated to pGEX-2T. *E. coli* transformed with these plasmids were induced with IPTG. Soluble, native GST fusion proteins were purified using a glutathione-resin and contained ~75% GST and 25% full-length GST–Nogo or GST–Rtn protein. Most of the GST–Nogo protein was not extractable under non-denaturing conditions, but an 8M-urea extract dialysed against PBS contained over 98% pure GST–Nogo.

Antibody production and immunohistology

Anti-Myc immunoblots and immunohistology with the 9E10 antibody were obtained as described[19,20]. The GST–Nogo fusion protein was used as an immunogen to generate an anti-Nogo rabbit antiserum. Antibody was affinity purified and used at 3 μg ml^{-1} for immunohistology and 1 μg ml^{-1} for immunoblots. To assess the specificity of the antiserum, staining was conducted in the presence of GST–Nogo protein at 0.1 mg ml^{-1}. For live-cell staining, cells were incubated in primary antibody dilutions at 4° for 1 hour in Hanks balanced salt solution with 0.05% (w/v) BSA and 20 mM Na-HEPES pH 7.3. After fixation, bound antibody was detected by incubation with fluorescently labelled secondary antibodies.

Messenger RNA distribution

For northern blots, total RNA on nylon membranes was hybridized with ^{32}P-labelled probes generated by the random priming method with the Klenow enzyme as described[21,22]. The 5′ Nogo probe corresponds to the nucleotides encoding residues 1–878, the 3′ Nogo probe to the entire Nogo-C coding sequence, and the Rtn3 probe to the entire coding sequence. *In situ* hybridization used the digoxegenin-labelled riboprobe method as described[21,22]. The 5′ Nogo, 3′ Nogo and Rtn3 riboprobes correspond to the same sequences used for northern blot probes. The Rtn1C riboprobes are complementary to the entire Rtn1C coding sequence.

Neural culture, growth cone collapse and neurite outgrowth

For the culture of embryonic chick E10 and E12 DRG explants and dissociated neurons, we used methods described for E7 DRG cultures[19–21,23]. Nerve growth factor-differentiated PC12 cells were cultured as described[24]. Embryonic spinal cord explants (rat E10 or chick E5) were cultured for 7–14 days in the presence of PDGF-AA to induce differentiation of some cells into mature oligodendrocytes[25]. The procedure for growth-cone-collapse assays is identical to that for analysis of Sema3A-induced growth cone collapse[19–21,23]. The method for analysis of total neurite outgrowth has also been described[21,23,24]. In outgrowth assays, proteins and peptides were added 1 hour after plating to minimize any effect on the total number of adherent cells. To test the effect of substrate-bound GST or GST–Nogo, the protein solutions were dried on poly-L-lysine coated glass, washed and then coated with laminin. For E12 cultures, the neuronal identity of cells was verified by staining with anti-neurofilament antibodies (2H3, Developmental Studies Hybridoma Bank) and neurites were traced by observation of rhodamine-phalloidin staining of F-actin in processes.

Received 12 November ; accepted 21 December 1999.

1. Benfy, M. & Aguayo, A. G. Extensive elongation of axons from rat brain into peripheral nerve grafts. *Nature* **296,** 150–152 (1982).
2. Schwab, M. E. & Thoenen, H. Dissociated neurons regenerate into sciatic but not optic nerve explants in culture irrespective of neurotrophic factors. *J. Neurosci.* **5,** 2415–2423 (1985).
3. Wang, L. H. *et al.* in *Neurobiology of Spinal Cord Injury* (eds Kalb, R. G. & Strittmatter, S. M.) 131–153 (Humana, Totowa, New Jersey, 1999).
4. Caroni, P. & Schwab, M. E. Two membrane protein fractions from rat central myelin with inhibitory properties for neurite growth and fibroblast spreading. *J. Cell Biol.* **106,** 1281–1288 (1988).
5. Spillmann, A. A., Bandtlow, C. E., Lottspeich, F., Keller, F. & Schwab, M. E. Identification and characterization of a bovine neurite growth inhibitor (bNI-220). *J. Biol. Chem.* **73,** 19283–19293 (1998).
6. McKerracher, L. *et al.* Identification of myelin-associated glycoprotein as a major myelin-derived inhibitor of neurite growth. *Neuron* **13,** 805–811 (1994).
7. Mukhopadhyay, G., Doherty, P., Walsh, F. S., Crocker, R. & Filbin, M. T. A novel role of myelin-associated glycoprotein as an inhibitor of axonal regeneration. *Neuron* **13,** 757–767 (1994).
8. Bregman, B. S. *et al.* Recovery from spinal cord injury mediated by antibodies to neurite growth inhibitors. *Nature* **378,** 498–501 (1995).
9. Thallmair, M. *et al.* Neurite growth inhibitors restrict plasticity and functional recovery following corticospinal tract lesions. *Nature Neurosci.* **1,** 24–31 (1998).
10. Nagase, T. *et al.* Prediction of the coding sequences of unidentified human genes. XII. The complete sequences of 100 new cDNA clones from brain which code for large proteins *in vitro*. *DNA Res.* **31,** 355–364 (1998).
11. van de Velde, H. J., Roebroek, A. J., Senden, N. H., Ramaekers, F. C. & Van de Ven, W. J. NSP-encoded reticulons, neuroendocrine proteins of a novel gene family associated with membranes of the endoplasmic reticulum. *J. Cell Sci.* **107,** 2403–2416 (1994).

12. Roebroek, A. J. *et al.* Genomic organization of the human NSP gene, prototype of a novel gene family encoding reticulons. *Genomics* **32,** 191–199 (1996).
13. Roebroek, A. J., Contreras, B., Pauli, I. G. & Van de Ven, W. J. cDNA cloning, genomic organization, and expression of the human RTN2 gene, a member of a gene family encoding reticulons. *Genomics* **51,** 98–106 (1998).
14. Moreira, E. F., Jaworski, C. J. & Rodriguez, I. R. Cloning of a novel member of the reticulon gene family (RTN3): gene structure and chromosomal localization to 11q13. *Genomics* **58,** 73–81 (1999).
15. Morris, N. J., Ross, S. A., Neveu, J. M., Lane, W. S. & Lienhard, G. E. Cloning and characterization of a new member of the reticulon family. *Biochim. Biophys. Acta* **1450,** 68–76 (1991).
16. Jackson, M. R., Nilsson, T. & Peterson, P. A. Identification of a consensus motif for retention of transmembrane proteins in the endoplasmic reticulum. *EMBO J.* **9,** 3153–3162 (1991).
17. Senden, N. H. *et al.* Neuroendocrine-specific protein C (NSP-C): subcellular localization and differential expression in relation to NSP-A. *Eur. J. Cell Biol.* **69,** 197–213 (1996).
18. Bandtlow, C. E. & Loschinger, J. Developmental changes in neuronal responsiveness to the CNS myelin-associated neurite growth inhibitor NI-35/250. *Eur. J. Neurosci.* **9,** 2743–2752 (1997).
19. Takahashi, T., Nakamura, F., Jin, Z., Kalb, R. G. & Strittmatter, S. M. Semaphorin A and E act as antagonists of neuropilin-1 and agonists of neuropilin-2 receptors. *Nature Neurosci.* **1,** 487–493 (1998).
20. Takahashi, T. *et al.* Plexin-neuropilin1 complexes form functional semaphorin-3A receptors. *Cell* **99,** 59–69 (1999).
21. Goshima, Y., Nakamura, F., Strittmatter, P. & Strittmatter, S. M. Collapsin-induced growth cone collapse mediated by an intracellular protein related to *unc*-33. *Nature* **376,** 509–514 (1995).
22. Wang, L. H. & Strittmatter, S. M. A family of rat CRMP genes is differentially expressed in the nervous system. *J. Neurosci.* **16,** 6197–6207 (1996).
23. Jin, Z. & Strittmatter, S. M. Rac1 mediates collapsin-induced growth cone collapse. *J. Neurosci.* **17,** 6256–6263 (1997).
24. Strittmatter, S. M., Fishman, M. C. & Zhu, X. P. Activated mutants of the α subunit of G_o promote an increased number of neurites per cell. *J. Neurosci.* **14,** 2327–2338 (1994).
25. Vartanian, T., Fischbach, G. & Miller, R. Failure of spinal cord oligodendrocyte development in mice lacking neuregulin. *Proc. Natl Acad. Sci. USA* **96,** 731–735 (1999).

Acknowledgements

The authors thank A. Fournier for invaluable experimental advice and assistance. This work was supported by grants to S.M.S. from the NIH and the American Paralysis Association, and to F.N. from the Spinal Cord Research Fund of the Paralyzed Veterans of America. S.M.S. is an Investigator of the Patrick and Catherine Weldon Donaghue Medical Research Foundation.

Correspondence and requests for materials should be addressed to S.M.S. (e-mail: stephen.strittmatter@yale.edu).

Torque-generating units of the flagellar motor of *Escherichia coli* have a high duty ratio

William S. Ryu*, Richard M. Berry† & Howard C. Berg*

* *Department of Molecular and Cellular Biology, Harvard University, 16 Divinity Avenue, Cambridge, Massachusetts 02138, USA and Rowland Institute for Science, 100 Edwin H. Land Boulevard, Cambridge, Massachusetts 02142, USA*
† *The Randall Centre, King's College London, London SE1 1UL, UK*

Rotation of the bacterial flagellar motor is driven by an ensemble of torque-generating units containing the proteins MotA and MotB[1–3]. Here, by inducing expression of MotA in *motA*$^-$ cells under conditions of low viscous load, we show that the limiting speed of the motor is independent of the number of units: at vanishing load, one unit turns the motor as rapidly as many. This result indicates that each unit may remain attached to the rotor for most of its mechanochemical cycle, that is, that it has a high duty ratio[4]. Thus, torque generators behave more like kinesin, the protein that moves vesicles along microtubules, than myosin, the protein that powers muscle. However, their translation rates, stepping frequencies and power outputs are much higher, being greater than 30 μm s^{-1}, 12 kHz and 1.5 × 10^5 pN nm s^{-1}, respectively.

Bacterial flagellar motors are driven by a transmembrane ion flux (reviewed in refs 5, 6). Most studies of their physiology have been done at low speeds, characteristic of high viscous loads, where translation rates of ions or movement of internal mechanical components are not limiting. To study their behaviour at higher speeds, we developed a new motor assay (Fig. 1a, inset). Instead of tethering a cell to a glass surface by a single flagellum and watching the cell body spin[7], we fixed the cell body to the glass surface and attached a polystyrene bead to a stub of one of its flagellar filaments. By using beads of various sizes (0.3–1 μm diameter), we could vary the load by a factor of more than 10. The bead was followed in a weak optical trap by back focal plane interferometry[8].

Figure 1a, b shows speed records for cells under high and low load, respectively. Upon induction of MotA expression, discrete increments in speed were observed. At high load (Fig. 1a), the increase in speed was linear with the torque-generator number, *N*, as observed previously with tethered cells[1,2]. However, at lower load (Fig. 1b), the speed tended to saturate at high torque-generator numbers. The data for different bead sizes are summarized in Fig. 2a. In Fig. 3a we show torque–speed curves for motors with between one and five torque-generating units, constructed from the data of Fig. 2a. At low speeds, the torque produced by a motor with *N* generators is simply *N* times the torque produced by a motor with one generator. At high speeds, the torques decline, and the curves are consistent with a limiting speed at zero torque of about 300 Hz.

The behaviour of the motor can be understood in terms of the 'duty ratio' of the torque generators[4], where the duty ratio, *D*, is defined as the fraction of time for which a generator is bound to the rotor. As the motor works against a viscous load, speed is proportional to the applied torque. At high loads, speed increases linearly with *N* whether *D* is small (close to 0) or large (close to 1). If *D* is small, the torque-generating units work independently of one another, because the probability that two might be attached at the same time is small; speed is proportional to the time-averaged torque. If *D* is large, each unit has time to reach thermodynamic equilibrium and exert the same torque; speed is proportional to the total torque. At vanishing load, speed increases linearly with *N* when

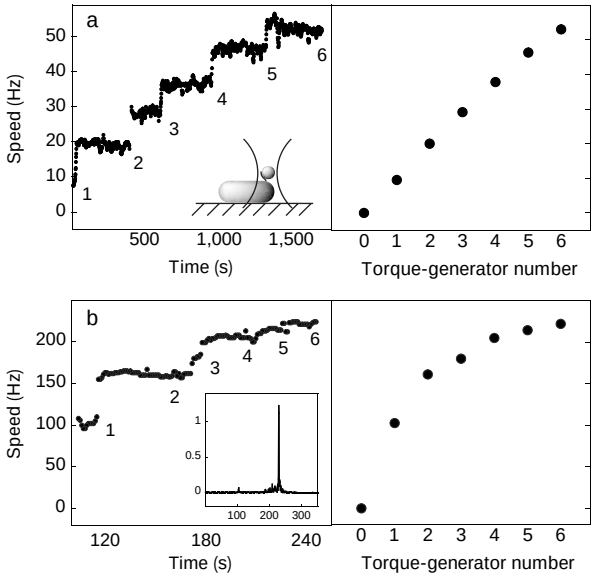

Figure 1 Measurements made at high and low load. **a**, Induction of torque in a motor driving a bead of 1.03 μm diameter (left). Speed is shown as a function of time, and the number of torque generators is indicated. Inset, a small bead attached to a segment of a flagellar filament and followed in a weak optical trap. Right, mean speed as a function of torque-generator number. Error bars are smaller than data markers. **b**, As in **a** for a different motor driving a bead of 0.30 μm diameter. Inset, the power spectrum of the signal from 80 revolutions of a 0.36-μm bead. The abscissa is frequency (Hz), and the ordinate is power (arbitrary units).